

# Hadron Physics at BaBar

David Muller  
Representing the BaBar Collaboration

*Stanford Linear Accelerator Center, Stanford, CA 94309, USA*

**Abstract.** The *BABAR* experiment at SLAC is designed to measure CP violation in the *B* meson system, however the very high statistics combined with the different  $e^+$  and  $e^-$  beam energies, the detector design and the open trigger allow a wide variety of spectroscopic measurements. We are beginning to tap this potential via several production mechanisms. Here we present recent results from initial state radiation, hadronic jets, few body *B* and *D* hadron decays, and interactions in the detector material. We also summarize measurements relevant to  $D_s$  meson spectroscopy, pentaquarks and charmonium spectroscopy from multiple production mechanisms.

**Keywords:** Initial State Radiation, Charm, Pentaquarks

**PACS:** 12.38.Qk, 13.66.Bc, 14.40.Lb

## INTRODUCTION

The *BABAR* program at SLAC is designed to measure CP violation in the *B* meson system by producing coherent  $B\bar{B}$  pairs and studying the time dependence of their decays into CP eigenstates. A 9 GeV electron beam and a 3.1 GeV positron beam collide at a center of mass energy of 10.58 GeV, corresponding to the peak of the  $Y(4S)$  resonance. The asymmetric *BABAR* detector covers about 85% of the solid angle in the  $e^+e^-$  center of mass (c.m.) frame, and is designed to isolate the low multiplicity *B* decays that occur in less than 0.001% of events through a combination of excellent charged particle tracking, charged hadron identification and photon detection.

These features are also beneficial for spectroscopy, and the very high luminosity required for CP violation studies yields very large samples of hadrons from hadronic jets and bottom (*B*) and charmed (*D*) hadron decays and allows us to study  $e^+e^-$  annihilations at lower  $\sqrt{s}$  through initial state radiation. Along with high luminosity come high backgrounds, and we are studying interactions of both beam halo and final state particles with the beampipe and detector material. These allow not only a good understanding of the detector itself, but also studies of  $e^\pm$  and long-lived hadron interactions with materials such as beryllium, tantalum, silicon, carbon and water.

Here we present an overview of our results in the area of hadron spectroscopy. Details can be found in these proceedings [1] and in the references. The first three sections discuss the three main production mechanisms we have used so far, and present a number of results. We follow with sections summarizing studies of  $D_s$  meson spectroscopy, pentaquarks, and charmonium spectroscopy that involve more than one of these mechanisms. We have accumulated over  $250 \text{ fb}^{-1}$  of data so far and expect at least four times this. These results thus constitute the beginning of an extremely rich program of spectroscopy at *BABAR*, and we look forward to many more results in the future.

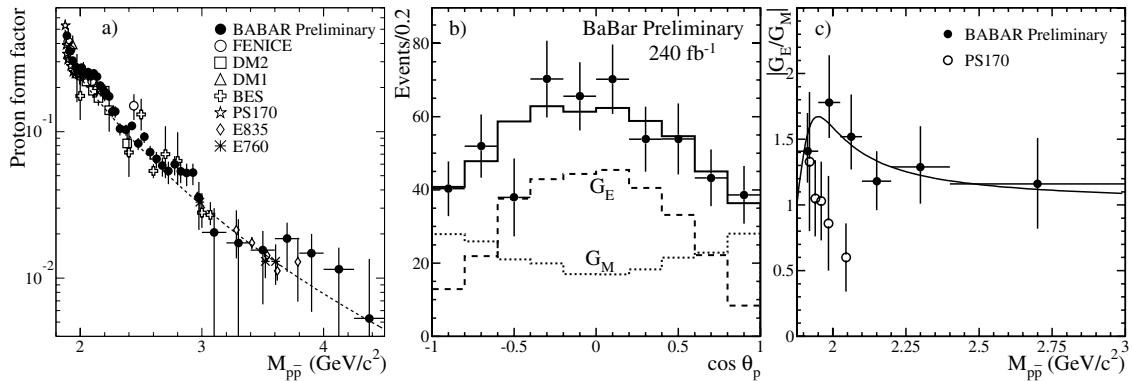


**FIGURE 1.** a) The effective proton form factor as a function of  $\sqrt{s}$  derived from our  $e^+e^- \rightarrow \gamma_{ISR}P\bar{P}$  data, compared with previous results. b) The proton angular distribution (points) for events in the range 1950–2025 MeV; the solid histogram represents a fit of the sum of electric (dashed) and magnetic (dotted) components. c) The ratio of electric and magnetic form factors as a function of  $\sqrt{s}$ .

## INITIAL STATE RADIATION

An  $e^+e^-$  pair can couple directly to any resonance with  $J^{(PC)} = 1^{--}$  and if a decay mode of that resonance can be reconstructed then the cross section as a function of  $\sqrt{s}$  in the vicinity of the resonance can be used to determine its mass, total width,  $e^+e^-$  width and width to that mode. We run 90% of the time at the peak of the  $\Upsilon(4S)$  resonance ( $\sqrt{s} = 10.58 \text{ GeV}$ ), 10% below the  $\Upsilon(4S)$  ( $\sqrt{s} = 10.54 \text{ GeV}$ ) to study non- $B\bar{B}$  backgrounds, and occasionally at other energies. Our total hadronic cross section yields improved values of the  $\Upsilon(4S)$  mass,  $10579.3 \pm 1.2 \text{ MeV}/c^2$ , total width,  $20.7 \pm 3.0 \text{ MeV}$ , and  $e^+e^-$  width,  $0.321 \pm 0.034 \text{ keV}$  [2].

Annihilations at lower  $\sqrt{s}$  can be studied via initial state radiation (ISR) events, in which one of the incoming leptons emits a photon and subsequently annihilates with the other. The cross section for this process is the product of the  $e^+e^-$  annihilation cross section at the reduced c.m. energy  $\sqrt{s'}$  and a well known radiator function; the latter falls rapidly with increasing photon energy, but the former increases at low  $\sqrt{s'}$  and becomes dominated by low multiplicity resonant contributions. By detecting the ISR photon, reconstructing a given final state and requiring overall 4-momentum conservation, we identify clean samples of ISR events and measure cross sections from threshold up to  $\sqrt{s'} = 4.5 \text{ GeV}$ . This includes the charmonium region, and we have improved measurements of the  $J/\psi$ , and sometimes  $\psi(2S)$ , branching fraction into each mode studied.

We have previously published [3] measurements of the  $\pi^+\pi^-\pi^0$ ,  $\pi^+\pi^-\pi^+\pi^-$ ,  $K^+K^-\pi^+\pi^-$  and  $K^+K^-\pi^+\pi^-$  final states with better coverage than all previous experiments and comparable or better precision, using  $89 \text{ fb}^{-1}$  of data. These states can be studied both in terms of cross section and internal structure. The  $\pi^+\pi^-\pi^0$  final state is dominated by  $\omega$  and  $\phi$  resonances, and we have improved the world's knowledge of excited  $\omega$  states. The  $\pi^+\pi^-\pi^+\pi^-$  final state is dominated by the two-body  $a_1(1260)\pi$  intermediate state; the  $K^+K^-\pi^+\pi^-$  final state shows no significant two-body states, but a rich three-body structure including  $K^*(890)K\pi$ ,  $\phi\pi\pi$ ,  $\rho KK$  and  $K_2^*(1430)K\pi$ ; the  $K^+K^-\pi^+\pi^-$  final state shows no substructure, in particular no  $\phi$  signal.

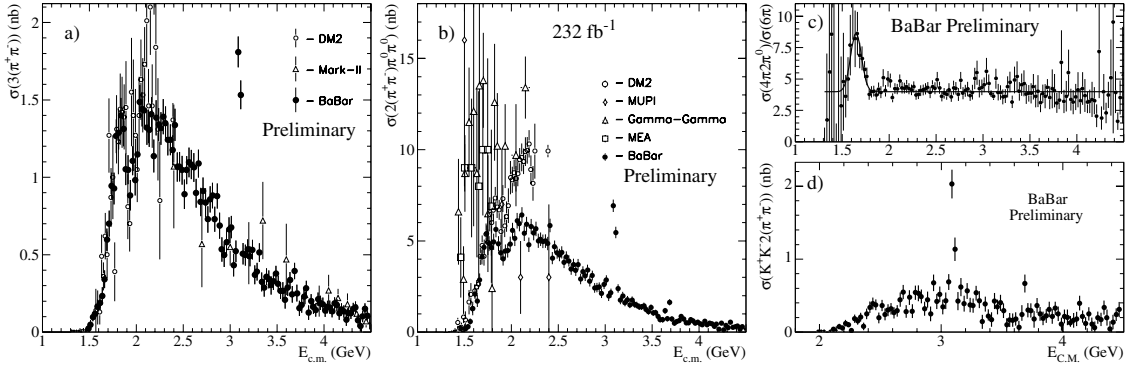


**FIGURE 2.** The cross section for  $e^+e^- \rightarrow$  a)  $\pi^+\pi^-\pi^+\pi^-\pi^+\pi^-$  and b)  $\pi^+\pi^-\pi^+\pi^-\pi^0\pi^0$  vs.  $\sqrt{s}$ , compared with previous data. c) The ratio of the cross sections in (a) and (b). d) The cross section for  $e^+e^- \rightarrow K^+K^-\pi^+\pi^-\pi^+\pi^-$ .

We have a preliminary measurement of the  $e^+e^- \rightarrow p\bar{p}$  cross section; the corresponding effective form factor is shown in Fig. 1a, along with previous data from  $e^+e^-$  and  $p\bar{p}$  experiments, with which we are consistent. The  $\sqrt{s'}$  dependence shows the familiar threshold enhancement, as well as two structures featuring sharp drops at 2.25 and 3 GeV, which illustrate the power of data from a single experiment over a wide range with no point-to-point systematic error. We separate the electric and magnetic form factors using the proton angular distribution, which is shown in Fig. 1b for the range  $1950 < \sqrt{s'} < 2025$  MeV; it deviates significantly from uniformity, indicating the electric form factor is substantially larger than the magnetic. The  $G_E:G_M$  ratio is shown as a function of  $\sqrt{s'}$  in Fig. 1c; the data show a systematic trend toward values above unity at low  $\sqrt{s'}$ , which is inconsistent with the LEAR data. The line in the figure is a parametrization used to calculate the effective form factor in Fig. 1a.

We also have preliminary studies of the  $\pi^+\pi^-\pi^+\pi^-\pi^+\pi^-$ ,  $\pi^+\pi^-\pi^+\pi^-\pi^0\pi^0$  and  $K^+K^-\pi^+\pi^-\pi^+\pi^-$  final states. The cross sections for the first two are shown in Figs. 2a,b; large improvements over previous measurements are evident. In the all-charged mode the structure around 1900 MeV seen previously by DM2 and also in diffractive production by FOCUS, is clear and well measured. There is surprisingly little substructure in this mode; a simulation with one  $\rho^0$  and four pions distributed according to phase space is adequate to describe all the internal distributions. The  $\pi^+\pi^-\pi^+\pi^-\pi^0\pi^0$  mode shows a rather similar cross section, but a much more complex internal structure: we observe signals for  $\rho^0$ ,  $\rho^\pm$ ,  $\omega$  and  $\eta$ , and a substantial contribution from the two-body  $\omega\eta$  intermediate state, which appears to be resonant. The ratio of the two cross sections is shown in Fig. 2c; the structure near 1650 MeV is due to the  $\omega\eta$  contribution, and the ratio is constant with a value near 4.0 over the remainder of the range, which is difficult to explain in light of the very different substructures. More data and modes containing more  $\pi^0$  are under study.

The  $K^+K^-\pi^+\pi^-\pi^+\pi^-$  cross section is measured for the first time and shown in Fig. 2d. There is interesting substructure, with a weak  $\phi$  signal, but a strong  $K^*(890)$ . More statistics and final states such as  $K^+K^-\pi^+\pi^-\pi^0\pi^0$  will be analyzed.

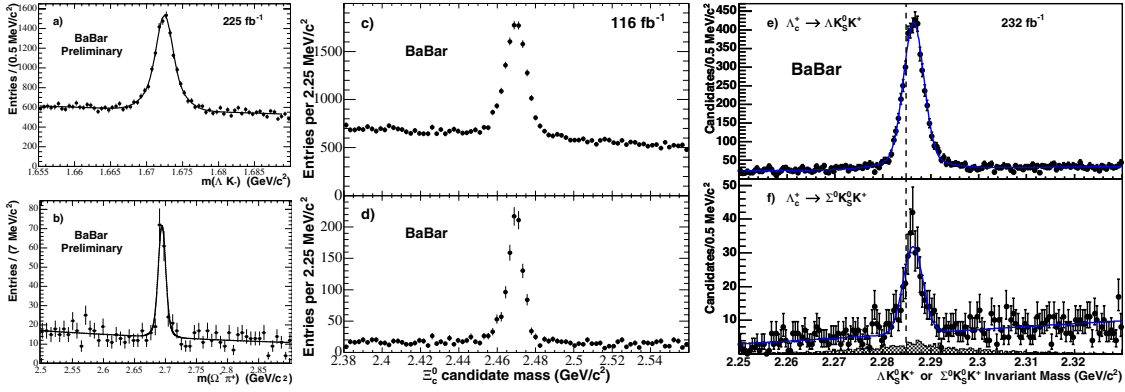


**FIGURE 3.** Inclusive a)  $\Lambda K^-$  and b)  $\Omega^- \pi^+$  invariant mass distributions in the vicinity of the  $\Omega^-$  and  $\Omega_c^0$ , respectively. Inclusive c)  $\Xi^- \pi^+$  and d)  $\Omega^- K^+$  invariant mass distributions in the vicinity of the  $\Xi_c^0$ . Inclusive e)  $\Lambda_c^+ \rightarrow \Lambda K_S^0 K^+$  and f)  $\Sigma^0 K_S^0 K^+$  invariant mass distributions in the vicinity of the  $\Lambda_c^+$ .

## HADRONIC JETS

Our most prevalent events are of the type  $e^+e^- \rightarrow q\bar{q}$  at  $\sqrt{s} = 10.58$  GeV, in which the quark and antiquark fragment into a number of hadrons, which produce typically ten stable charged tracks and photons. This process is not understood quantitatively, so there is no quantum number information from the production process; however states sufficiently narrow to be seen above background can yield masses, widths and branching fractions, and some quantum numbers can be excluded by observed decay modes.

Our samples of reconstructed hyperons, e.g.  $\Lambda^0$ ,  $\Sigma^0$ ,  $\Xi^{0,-}$ ,  $\Omega^-$  (Fig. 3a),  $\Xi(1530)$ , are much larger and cleaner than in pre- $B$ -factory  $e^+e^-$  experiments. These signals have numerous applications, such as the study of charmed baryons from  $c\bar{c}$  events and  $B$  hadron decays. For  $\Xi^- \pi^+$  and  $\Omega^- K^+$  pairs we show distributions of invariant mass  $M(\Xi^- \pi^+)$  and  $M(\Omega^- K^+)$  in Figs. 3c and 3d, respectively; both show clear signals for the charmed-strange baryon  $\Xi_c(2470)^0$  and we measure the branching ratio  $\mathcal{B}(\Xi_c^0 \rightarrow \Omega^- K^+) / \mathcal{B}(\Xi_c^0 \rightarrow \Xi^- \pi^+) = 0.294 \pm 0.024$  [4]. We also observe the doubly strange, charmed baryon  $\Omega_c(2700)^0$  in the  $M(\Omega^- \pi^+)$  distribution shown in Fig. 3b. Signals for other decay modes are not yet significant, but we measure [5] (preliminary)

$$\begin{aligned} \mathcal{B}(\Omega_c^0 \rightarrow \Xi^- K^- \pi^+ \pi^+) / \mathcal{B}(\Omega_c^0 \rightarrow \Omega^- \pi^+) &= 0.31 \pm 0.15 \\ \mathcal{B}(\Omega_c^0 \rightarrow \Omega^- \pi^+ \pi^- \pi^+) / \mathcal{B}(\Omega_c^0 \rightarrow \Omega^- \pi^+) &= 0.16 \pm 0.10. \end{aligned}$$

We measure the mass of the  $\Lambda_c^+$  baryon using the  $\Lambda K_S^0 K^+$  and  $\Sigma^0 K_S^0 K^+$  decay modes. These have low  $Q$  values (and therefore low branching fractions), which minimize the systematic error due to uncertainties in the mass scale and resolution of the detector. The invariant mass distributions for these two modes are shown in Figs. 3e and 3f; the former mode contains over 4,000 true  $\Lambda_c^+$  baryons and the mass measurement is systematics limited; the latter mode has a smaller systematic error, but is statistics limited. The masses measured in the two modes are consistent and the combined result,  $M_{\Lambda_c} = 2286.46 \pm 0.14$  MeV/ $c^2$  [6], is four times more precise than the current PDG value of  $2284.9 \pm 0.6$  MeV/ $c^2$  [7] and higher by 2.5 of the PDG standard deviations.

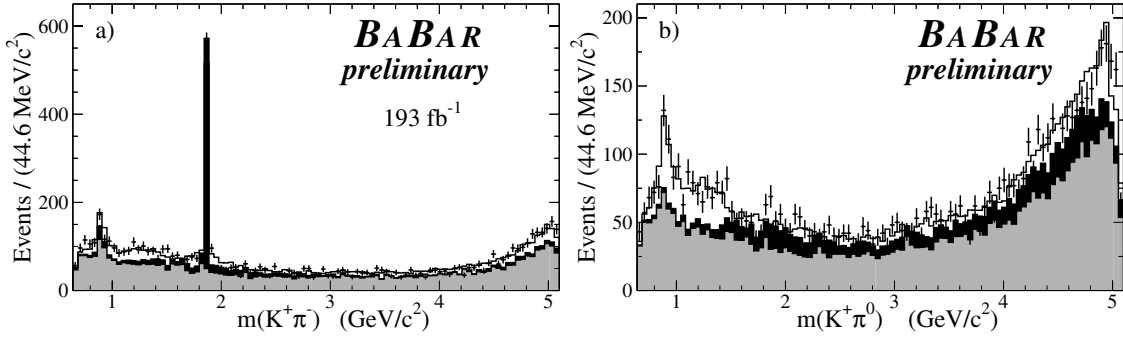


**FIGURE 4.** The a)  $K^+\pi^-$  and b)  $K^+\pi^0$  invariant mass distributions in selected  $B^0 \rightarrow K^+\pi^-\pi^0$  candidates (points with error bars). The gray areas represent the combinatoric background from  $e^+e^-$  annihilations into hadrons, and the black areas the contributions from other  $B$  meson decays, including the  $B^0 \rightarrow \bar{D}^0\pi^0$  intermediate state. The histograms represent the result of a fit.

## B AND D HADRON DECAYS

The weakly decaying  $B$  and  $D$  hadrons are pseudoscalars, with their (quasi-)two-body decays limited to appropriate quantum numbers and helicity states. These uncommon, low-multiplicity decays can be sensitive to CP-violation, and are the goal of our program. We often use "applied spectroscopy", e.g. using angular distributions to reduce backgrounds or project out CP-even and CP-odd components. Recently we improved our measurement [8] of CP violation in  $B^0 \rightarrow J/\psi K^{*0}$  decays, including a full analysis of the  $J/\psi K\pi$  system. We see phase motion around  $890 \text{ MeV}/c^2$ , the direction of which resolves a sign ambiguity in the cosine of the CP-violating phase, and the S-P phase difference agrees with corresponding LASS data from  $K^-p \rightarrow K^-\pi^+n$  scattering.

Dalitz analyses of three-body modes can supply a wealth of spectroscopic information. We have analyzed several  $D$  meson decays with much higher statistics than earlier experiments, and are starting to study decays of the much heavier  $B$  mesons, both for their own sake and to maximize CP information. We have preliminary results for  $B^0 \rightarrow K^+\pi^-\pi^0$ ,  $B^+ \rightarrow K^+\pi^-\pi^+$  and  $B^+ \rightarrow \pi^+\pi^-\pi^+$  [9]. The  $M(K^+\pi^-)$  and  $M(K^+\pi^0)$  projections for the former are shown in Fig. 4. The background from  $e^+e^- \rightarrow q\bar{q}$  events is large but measurable in off-resonance data. The background from other  $B$  meson decays can be more complicated: here we consider  $B^0 \rightarrow \bar{D}^0\pi^0$  as background, since the  $\bar{D}^0$  decays weakly and its mass projections are calculable; the remaining  $B$  decay background is suppressed strongly by the selection criteria, but must be modelled.

These data yield qualitative information on the internal structure of this decay. Both  $K\pi$  systems are dominated by S-wave components, with  $K_0^*(1430)\pi$  amplitudes 3–4 times the  $K^*(890)\pi$  amplitudes. In the  $\pi^-\pi^0$  system there is a substantial  $\rho^-$ , but S-wave resonances should be suppressed by isospin. In the  $B^+ \rightarrow K^+\pi^-\pi^+$  decay we observe S-wave dominance, with the  $K_0^*(1430)^0\pi^+$  amplitude being  $\sim 5$  times larger than that of the  $K^*(890)^0\pi^+$  and the  $K^+f_0(980)$  being about twice the  $K^+\rho^0(770)$ . On the other hand, in the  $B^+ \rightarrow \pi^+\pi^-\pi^+$  decay we observe large contributions from  $\rho(770)^0\pi^+$ ,  $\rho(1450)^0\pi^+$  and  $f_2(1270)^0\pi^+$ , but no significant S-wave contribution.

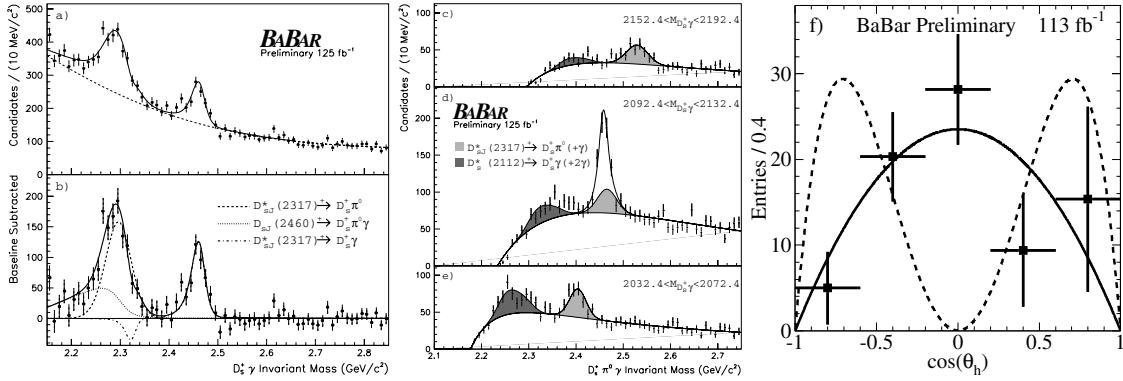


**FIGURE 5.** The inclusive  $D_s(1968)\gamma$  invariant mass distribution a) before and b) after subtraction of combinatorial background. The lines represent the results of a fit to the data with the components indicated. c,d,e) The inclusive  $D_s(1968)\pi^0\gamma$  invariant mass distribution in three ranges of the  $D_s(1968)\gamma$  submass. The lines (gray areas) represent the results of a fit to the data (contributions from the indicated feed-ups). f) The distribution of the cosine of the helicity angle for decays of  $D_{sJ}(2460) \rightarrow D_s\gamma$  in  $B^0 \rightarrow \bar{D}D_{sJ}(2460)$  decays; the solid (dashed) line represents the expectation for the spin-1 (spin-2) hypothesis.

## $D_S$ MESON SPECTROSCOPY

The  $D_s^+$  mesons are bound states of a ‘heavy’ charmed quark and a ‘medium’ mass strange antiquark and their spectrum provides an interesting theoretical testing ground. Prior to the  $B$  factories, four narrow states were known, with masses of 1968, 2112, 2536 and 2573  $\text{MeV}/c^2$ , and assigned to the expected narrow states with respective  $J^P = 0^-, 1^-, 1^+$  and  $2^+$ , although the spins of the latter three states are unmeasured. The low-mass  $0^+$  and  $1^+$  states were expected to be wide and to lie above  $DK$  and  $D^*K$  thresholds, respectively, so it was surprising when two narrow states,  $D_{sJ}(2317)$  and  $D_{sJ}(2460)$ , were discovered in the isospin violating decay modes  $D_s(1963)\pi^0$  and  $D_s^*(2112)\pi^0$ . These discoveries reinvigorated both experiment and theory in this area, with abundant theoretical speculation that they may not be simple  $c\bar{s}$  states, but perhaps 4-quark states,  $DK$  ‘molecules’ or ‘hybrid’  $c\bar{s}g$  states. It is of great importance to establish their quantum numbers experimentally.

The observation of specific additional states or decay modes can exclude certain hypotheses, and we have done a number of studies [10]. In the  $D_s(1968)\pi^\pm$  invariant mass spectra we find no evidence for the neutral or doubly charged states that would be expected as isospin partners of any molecular state. In the inclusive  $D_s(1968)\pi^-\pi^+$  invariant mass distribution we observe signals at 2460 and 2536  $\text{MeV}/c^2$ , excluding the  $0^+$  hypothesis for those states; there is no signal at 2317  $\text{MeV}/c^2$ .

We have searched for radiative decays to  $D_s(1963)\gamma$  and  $D_s(1963)\gamma\pi^0$ , in which there is considerable cross-feed to be taken into account. In Figs. 5a and 5b we show the inclusive  $D_s^+\gamma$  invariant mass distribution before and after subtraction of the combinatorial background, respectively, and in Figs. 5c,d,e we show the inclusive  $D_s^+\gamma\pi^0$  invariant mass distribution in three ranges of the  $D_s^+\gamma$  submass. There is a signal for  $D_{sJ}(2460) \rightarrow D_s^+\gamma$  in Fig. 5a,b, however the structure at lower mass is due to a combination of feeddowns from  $D_{sJ}(2460)$  decays and  $D_{sJ}(2317) \rightarrow D_s^+\pi^0$  decays where

only one of the photons from the  $\pi^0$  is found. Feed-up from  $D_{sJ}(2317) \rightarrow D_s^+ \pi^0$  and  $D_s^*(2112) \rightarrow D_s^+ \gamma$  with additional photons attached gives rise to the structures in gray in Figs. 5c,d,e that move with the the  $D_s^+ \gamma$  submass. A signal is seen at 2460 MeV/ $c^2$  only in Fig. 5d, indicating that the  $D_{sJ}(2460) \rightarrow D_s^+ \gamma \pi^0$  decay proceeds almost entirely through the  $D_s^*(2112) \pi^0$  intermediate state. These data confirm the exclusion of the spin-0 hypothesis for the  $D_{sJ}(2460)$  and suggest the  $D_{sJ}(2317)$  has spin 0.

These studies reveal the limitations of working with production in  $e^+ e^- \rightarrow c \bar{c}$  events. We have also studied  $D_{sJ}$  production in exclusive  $B$  decays [11], finding evidence for both the 2317 and 2460 states in several  $B \rightarrow \bar{D}^{(*)} D_{sJ}$  modes. These signals have lower statistics but also much lower background and provide complementary information on masses and branching ratios. In particular we obtain an improved value of  $\mathcal{B}(D_{sJ}(2460)^+ \rightarrow D_s \gamma) / \mathcal{B}(D_{sJ}(2460)^+ \rightarrow D_s^* \pi^0) = 0.27 \pm 0.05$ . Since the  $B$  and  $D$  are both pseudoscalars, the  $B \rightarrow \bar{D} D_{sJ}$  decays can be used to measure the spin of the  $D_{sJ}$  directly. The distribution of the cosine of the angle  $\theta_h$  between the  $D_s$  flight direction and the  $\bar{D}$  flight direction in the  $D_{sJ}(2460)$  rest frame is shown in Fig 5f, along with the expectations for the spin-1 and spin-2 hypotheses. Statistics are low, but the data show a strong preference for spin-1 over spin-2 (or any higher spin).

## PENTAQUARKS

The claims for the exotic baryonic states  $\Theta(1540)^+$ ,  $\Xi(1860)^{--}$  and  $\Theta_c(3100)^0$  generated strong interest in *BABAR* because of the small widths and the expectation of a large number of additional narrow states. In contrast to fixed target experiments,  $e^+ e^-$  annihilations produce all members of a given multiplet at about the same rate, giving access to more states. The production rate of such 5-quark states in  $e^+ e^-$  annihilations is unknown, but ordinary baryons are observed at rates decreasing exponentially with mass, and we observe large samples of baryons with masses above 1540 MeV/ $c^2$ , so we should be able to provide useful information as to the nature of these states.

Extensive searches [12] in our inclusive  $e^+ e^- \rightarrow q \bar{q}$  and  $Y(4S)$  data for the  $\Theta(1540)^+$ ,  $\Xi(1860)^{--}$  and other states in the antidecuplet generally supposed to contain them yield no signals. We limit their production rates to factors of 5–15 below the corresponding rates for baryons of the same mass, strongly suggesting that these states cannot be ordinary baryons. A preliminary search for the charmed exotic state  $\Theta_c(3100)^0$  claimed by the H1 collaboration, using the same  $p D^{*-}$  decay mode, is shown in Fig. 6a. Our mass resolution is  $\sim 3$  MeV/ $c^2$ , and there is no evidence for any narrow structure; in particular the region near 3100 MeV/ $c^2$  (inset) is smooth. Few charmed baryon rates have been measured, so we cannot draw the same conclusion as for the non-charmed states; however our  $D^{*-}$  sample is two hundred times larger than H1's, so we can exclude that their signal arises from either of the sources to which we are sensitive, hard  $c$ -quark fragmentation or  $B$  hadron decay.

We search for exotic states in several exclusive  $B$  hadron decays, finding no signal. For example, in [13] we study  $B^+ \rightarrow p \bar{p} K^+$  decays, observing a threshold enhancement in  $M(p \bar{p})$ , the  $\eta_c K^+$ ,  $J/\psi K^+$  and  $\psi(2S) K^+$  intermediate states, and evidence for the  $\chi_c K^+$  and  $p \bar{\Lambda}(1520)$  intermediate states. We see no other structure, such as the excess in

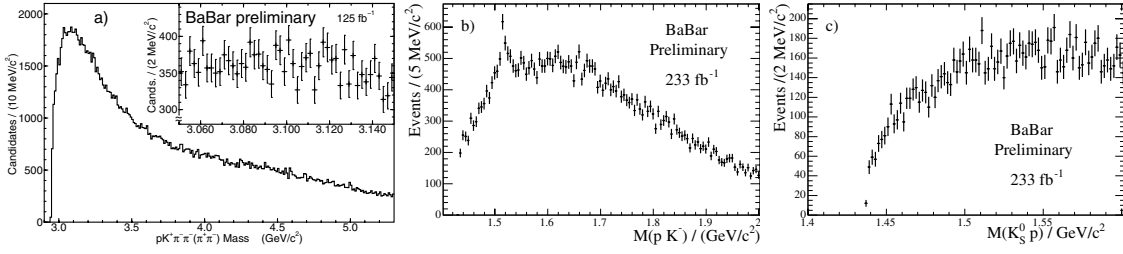


**FIGURE 6.** a) The inclusive  $pD^{*-}$  invariant mass distribution over the full kinematic range and (inset, with suppressed zero) in the vicinity of  $3100 \text{ MeV}/c^2$ . The b)  $pK^-$  and c)  $pK_S^0$  invariant mass distributions for  $pK_S^0 K^-$  combinations forming a vertex in the beampipe or detector material.

$M(pK^+)$  near  $1650 \text{ MeV}/c^2$  predicted for an excited  $\Theta$  multiplet, and we set a stringent limit on  $\Theta^{*++}$  production in  $B$  decays.

These negative results do not exclude these states' existence, so we search for hadro- and electro-production of  $\Theta(1540)^+$  in our beampipe and detector material. Along with high luminosity come high backgrounds from final state particles and off-momentum beam particles interacting in this material. A study of  $pK_S^0$  vertices gives a detailed inner detector map, and we can isolate interactions in Be, Si, Ta, Fe and C. The largest contribution of over 300,000 vertices from  $\sim 9 \text{ GeV}$  electrons hitting the Be of the beampipe constitutes an electroproduction experiment rather similar to several of the experiments claiming a signal. An observation here, combined with the non-observation in  $e^+e^-$  annihilations by the same experiment would be decisive.

We see no signal for the  $\Theta(1540)^+$  in the  $M(pK_S^0)$  spectrum for any type of interaction. We isolate more exclusive reactions by rejecting events in which another track identified as a proton, deuteron or triton can be attached to the  $pK_S^0$  vertex. In vertices with an associated  $\pi^\pm$ , we observe  $K^*(890)^+ \rightarrow K_S^0 \pi^+$ ,  $K^*(890)^- \rightarrow K_S^0 \pi^-$  and  $\Lambda \rightarrow p\pi^-$ , but no structure in the  $M(pK_S^0)$  distribution. We consider vertices with an associated  $K^-$ ; if no other strange particle is produced in such an event, then the  $K_S^0$  must have been a  $K^0$  rather than a  $\bar{K}^0$  and the  $pK_S^0$  combination is exotic. The  $M(pK^-)$  distribution in such events is shown in Fig. 6b; a signal for  $\Lambda(1520)$  is evident. The  $M(pK_S^0)$  distribution in the same events, Fig. 6c, shows no signal near  $1540 \text{ MeV}/c^2$ .

## CHARMONIUM SPECTROSCOPY

The field of charmonium spectroscopy has also been revitalized with the observations of the  $\eta_c(2S)$  and  $h_c$  states below  $D\bar{D}$  threshold, the discovery of the  $X(372)$  state well above  $D\bar{D}$  threshold but decaying to  $J/\psi\pi^+\pi^-$ , and the discovery of states at  $3940 \text{ MeV}/c^2$  in three different production processes decaying into non- $D\bar{D}$  modes. Theoretical models predict numerous wide charmonium states above  $D\bar{D}$  threshold, but the only experimental data, from the total hadronic cross section in  $e^+e^-$ , show only broad structures and the need for at least three states. Again there is speculation regarding molecules, hybrids, etc. To improve the situation, further experimental searches and systematic studies of the spectrum in different production processes are needed.

We set a stringent limit on  $X(372)$  production via ISR [3], strongly disfavoring the



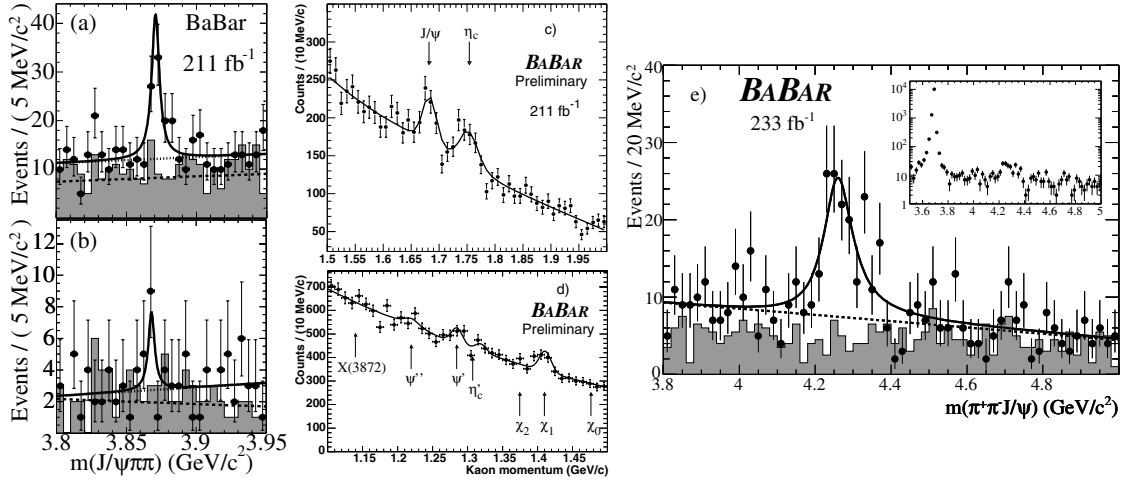


**FIGURE 7.** Invariant mass distributions for the  $J/\psi\pi^+\pi^-$  system in candidate a)  $B^+ \rightarrow J/\psi\pi^+\pi^-K^+$  and b)  $B^0 \rightarrow J/\psi\pi^+\pi^-K_S^0$  decays, in the vicinity of  $3870 \text{ MeV}/c^2$ . The lines represent the results of a fit. The  $K^+$  momentum spectrum in the rest frame of the system recoiling against a reconstructed  $B^-$  candidate, in the ranges corresponding to c)  $B^+ \rightarrow J/\psi K^+$  and  $B^+ \rightarrow \eta_c K^+$  decays and d)  $B^+$  decays to a  $K^+$  and a higher charmonium resonance. e) The  $J/\psi\pi^+\pi^-$  invariant mass distribution for ISR events in the vicinity of  $4300 \text{ MeV}/c^2$  and (inset) on a log scale over a wider range that includes the  $\psi(2S)$ .

$1^{--}$  hypothesis. We do observe it [14] in the decay  $B^+ \rightarrow X(3872)K^+ \rightarrow J/\psi\pi^+\pi^-K^+$ , as shown in Fig. 7a. The analogous neutral decay  $B^0 \rightarrow X(3872)K_S^0 \rightarrow J/\psi\pi^+\pi^-\pi^+\pi^-$  has the potential to discriminate between a number of models: if the  $X(3872)$  is a conventional  $c\bar{c}$  state, the two decays should have the same rate, although lower experimental acceptance reduces the expected number of the latter to about ten; molecular models predict a suppression of the latter decay; diquark-antidiquark models predict equal rates, but with the observed  $X$  mass shifted by about  $8 \text{ MeV}/c^2$  in the latter case. Our  $M(J/\psi\pi^+\pi^-)$  distribution [14] in these decays is shown in Fig. 7b. Current data are consistent with all three of these hypotheses; the best fit, indicated by the line, corresponds to a signal of about seven events with a mass lower by about  $3 \text{ MeV}/c^2$ .

In a new study of charmonium from  $B$  decays, we search for all  $B^+ \rightarrow K^+X_{c\bar{c}}$  decays by reconstructing the accompanying  $B^-$  in the event and measuring the  $K^+$  momentum spectrum in the rest frame of the  $B^+$ . We thus measure the absolute branching fractions of the  $B$  decays, independent of the  $X_{c\bar{c}}$  decay mode, which can be used along with existing data to improve our knowledge of a number of other branching fractions and decay widths. The kaon momentum spectrum is shown in Figs. 7c,d after a selection that enhances quasi-two-body decays and has been optimized separately in the two mass regions shown. There are signals for  $X_{c\bar{c}} = J/\psi, \eta_c, \chi_{c1}$ , and  $\psi(2S)$ , as well as enhancements corresponding to  $\eta_c(2S)$  and  $\psi(3770)$ . The observed suppression of  $\chi_{c0}$  and  $\chi_{c2}$  is predicted by factorization models. We see no evidence for  $h_c$  production, although the uncertainty is large due to its proximity to the  $\chi_{c1}$ . We see no signal for the  $X(3872)$ ; since we have observed the corresponding exclusive decay, we set a *lower* limit of  $\mathcal{B}(X(3872) \rightarrow J/\psi\pi^+\pi^-) > 4\%$  at the 90% C.L. No additional states are observed; the region above the  $X(3872)$  corresponds to  $K^+$  momenta below  $1.1 \text{ GeV}/c$  where the background increases rapidly, and is under study.

We verify [15] the Belle result that the exclusive process  $e^+e^- \rightarrow X_{c\bar{c}}X'_{c\bar{c}}$ , where  $X_{c\bar{c}}$  and  $X'_{c\bar{c}}$  are two charmonium states, has a much higher rate than expected when  $X_{c\bar{c}} = J/\psi$  or  $\psi(2S)$  and  $X'_{c\bar{c}} = \eta_c, \chi_{c0}$  or  $\eta_c(2S)$ . In addition we study the exclusive process  $e^+e^- \rightarrow J/\psi\pi^+\pi^-$  using ISR [16]; here we do not require a detected ISR photon since leptonic  $J/\psi$  decays plus missing mass requirements produce a clean signal, but we verify the expected rate and angular distribution of associated photons. The raw number of selected events is shown vs.  $M(J/\psi\pi^+\pi^-)$  in Fig. 7e on both linear and (inset) logarithmic vertical scales; in the latter the signal for  $\psi(2S)$ , a vital control mode, is prominent; in the former there is an excess of events near 4260 MeV/ $c^2$ , which we designate the  $Y(4260)$ . With the current statistics we are unable to determine if this is a single resonance or a more complex structure. If one resonance, its width is  $\sim 90$  MeV; such a state is expected to decay strongly to  $D\bar{D}$  and contribute to the total hadronic cross section, whereas the measured cross section is low in this mass region.

## SUMMARY

The excellent detector performance and high statistics in many different production processes makes *BABAR* an exciting place to do spectroscopy. We have already produced results in a number of areas, including  $e^+e^-$  annihilations at  $\sqrt{s}$  from  $\pi^+\pi^-$  threshold up to 4.5 GeV using ISR, charmed hadrons produced in  $e^+e^- \rightarrow c\bar{c}$  events and  $B$  hadron decays, Dalitz analyses of three-body  $B$  and  $D$  hadron decays, and analyses of interactions in the beampipe and detector material.

With CLEO and Belle, we have revitalized fields of  $c\bar{c}$  spectroscopy, with the discovery of the  $D_{sJ}(2317)$  and  $D_{sJ}(2460)$  states, and charmonium spectroscopy, with the observation of several new states, most recently our  $Y(4260)$ , and the development of inclusive methods such as  $B \rightarrow KX_{c\bar{c}}$ ,  $e^+e^- \rightarrow X_{c\bar{c}}X'_{c\bar{c}}$ , and ISR in specific final states such as  $J/\psi\pi^+\pi^-$ . We played a strong role in the pentaquark controversy, and look forward to a long and fruitful program in these and additional exciting areas.

## REFERENCES

1. N. Berger, T. Berger-Hrynova, V. Poireau, M. Negrini and V. Ziegler, these proceedings.
2. B. Aubert, et al., hep-ex/0405025, submitted to Phys. Rev. Lett.
3. B. Aubert, et al., Phys. Rev. **D70**, 072004 (2004), Phys. Rev. **D71**, 052001 (2004).
4. B. Aubert, et al., Phys. Rev. Lett. **95**, 142003 (2005).
5. B. Aubert, et al., hep-ex/0507011.
6. B. Aubert, et al., hep-ex/0507009, submitted to Phys. Rev. **D**.
7. Particle Data Group, S. Eidelman, et al., Phys. Lett. **B 592**, 1 (2004).
8. B. Aubert, et al., Phys. Rev. **D71**, 032005 (2004).
9. B. Aubert, et al., hep-ex/0408088; hep-ex/0507004 and hep-ex/0507025, submitted to Phys. Rev. **D**.
10. B. Aubert, et al., hep-ex/0408067.
11. B. Aubert, et al., Phys. Rev. Lett. **93**, 181801 (2004).
12. B. Aubert, et al., Phys. Rev. Lett. **95**, 042002 (2005); hep-ex/0408064.
13. B. Aubert, et al., Phys. Rev. **D72**, 051101(R) (2005).
14. B. Aubert, et al., hep-ex/0507090, submitted to Physical Review Letters.
15. B. Aubert, et al., Phys. Rev. **D72**, 031101 (2005).
16. B. Aubert, et al., Phys. Rev. Lett. **95**, 142001 (2005).